



Effect of deep drawing on the performance of coil-coatings assessed by electrochemical techniques

A.C. Bastos¹, A.M.P. Simões*

ICEMS/DEQB, Instituto Superior Técnico, TULisbon, Av. Rovisco Pais, 1049-001 Lisboa, Portugal

ARTICLE INFO

Article history:

Received 18 April 2008

Received in revised form 31 October 2008

Accepted 9 January 2009

Keywords:

Coil-coatings

Corrosion

EIS

Mechanical deformation

ABSTRACT

The effect of forming on the corrosion performance of coil-coated galvanised steel is studied. The study was made using the deep drawing geometry and the corrosion behaviour of formed and non-formed samples was compared, using electrochemical impedance spectroscopy (EIS). The responses of the various layers (zinc, phosphate and organic film) were observed separately. Formed samples suffer much faster degradation, in the form of blisters or of total delamination for phosphated and non-phosphated systems, respectively. The drop in the resistance values caused by forming in the phosphated samples revealed a transition from passive to active, whereas in the non-phosphated material the loss of resistance corresponds to an acceleration of the corrosion processes. The choice of the best equivalent circuits describing the impedance response is discussed.

© 2009 Elsevier B.V. All rights reserved.

1. Introduction

Steel in sheet form is very versatile and over one-third of the annual steel production is converted to this form [1]. Corrosion resistance of steel sheet is greatly increased when metallic and organic coatings are applied together [2]. In recent decades this concept was extended to *coil-coating* or pre-painted metal sheet, whose key idea is that flat surfaces are easier to coat than irregular shapes. A continuous metal sheet is cleaned, pre-treated and painted sequentially under strict quality control. As a consequence of this production process, specifications of the final coil are reproducible, the waste of paint is almost negligible, the solvent release is controlled and the energetic costs are optimised. On the other hand, coil-coatings are difficult to weld, prone to cut-edge corrosion and the shaping process may introduce micro-defects. The final manufacturer will uncoil, cut and shape the sheet to the desired form. Forming processes such as bending, drawing and deep drawing, produce articles with uneven strain distributed along their surfaces. Being employed mainly as exterior cover of appliances and buildings, coil-coatings have an important aesthetic function, and some properties, such as gloss, are very sensitive to the surface roughness induced by strain. Cosmetic corrosion is usually the most important type of corrosion, since the material is replaced long before it poses a structural or functional risk.

Aiming at a better understanding of the effect of mechanical deformation on the properties of coil-coatings, several researchers have dedicated efforts to the study of these materials, mostly using mechanical methods. Lange et al. [3] studied the formation and effects of scratches and abrasion during the forming process and in the service life of coil-coated steel. Kim et al. [4] investigated the forming and friction characteristics of several coil-coated systems on die materials. Ueda et al. [5] compared the response of the complete coated system with the response of the free paint films.

Less known is the effect of forming on the anticorrosive resistance of coil-coatings. Industrial tests are frequently based upon accelerated corrosion chambers, where visual inspection and delamination from artificial scribes grant a fast but empirical way of ranking the corrosion performance. One of the preferred types of sample is the deep-drawn cup, as it mimics real-life objects with complex geometries. In terms of research, publications are scarce. Deflorian et al. [6] studied polyester systems formed by bending and by the cupping test. Lavaert et al. [7] investigated the effect of uniaxial elongation and bending. Barbucci and coworkers used T-bend formed samples to optimise and select different coil-coated systems [8]. In our group, work has been undertaken measuring the water uptake of systems after bending and after the Erichsen test [9], and studying samples under uniaxial, biaxial and plane strain [10,11]. All of these investigations have evidenced the use of electrochemical impedance spectroscopy (EIS) for evaluation of corrosion resistance. Naturally, the pre-treatment plays an important role in the loss of adhesion and corrosion progression. One common practice in terms of pre-treatment is phosphating, which is known to improve paint adhesion [12].

* Corresponding author. Tel.: +351 218417963; fax: +351 218419771.

E-mail address: alda.simoes@ist.utl.pt (A.M.P. Simões).

¹ Present address: University of Aveiro, Dept. Ceramics and Glass Engineering, 3810-193 Aveiro, Portugal.

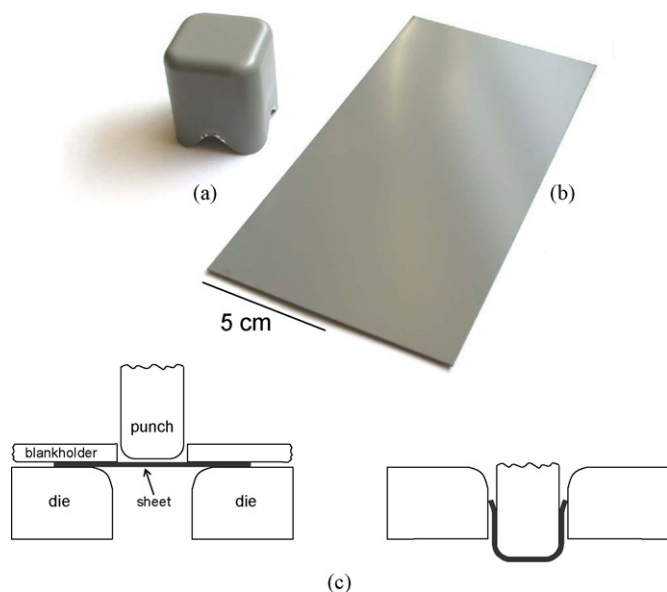


Fig. 1. Formed (a) and flat (b) samples; deep-drawing scheme (c).

In this work, deep drawn samples were tested by EIS in order to obtain more quantitative information on their degradation. Flat, unformed panels were included for comparison. The coil-coating used was either pre-treated (phosphated) or untreated.

2. Experimental

2.1. Materials and samples

A steel manufacturer produced the coil-coated material in a pilot plant, in order to guarantee reproducibility and consistency for all tested samples. The base material consisted on 800- μm thick DC04 steel [13] with a 7 μm layer of electrodeposited zinc. The surface was either alkaline degreased (EG, electrogalvanised steel) or pre-treated by a phosphating process followed by a rinse in a chromate solution (PEG, phosphated electrogalvanised steel). The paint system consisted of a 5 μm polyester primer plus a 15 μm polyurethane intercoat and no topcoat was used, in order to accelerate tests. Samples were either flat panels or formed samples produced by rectangular deep drawing (four corner cups) – Fig. 1.

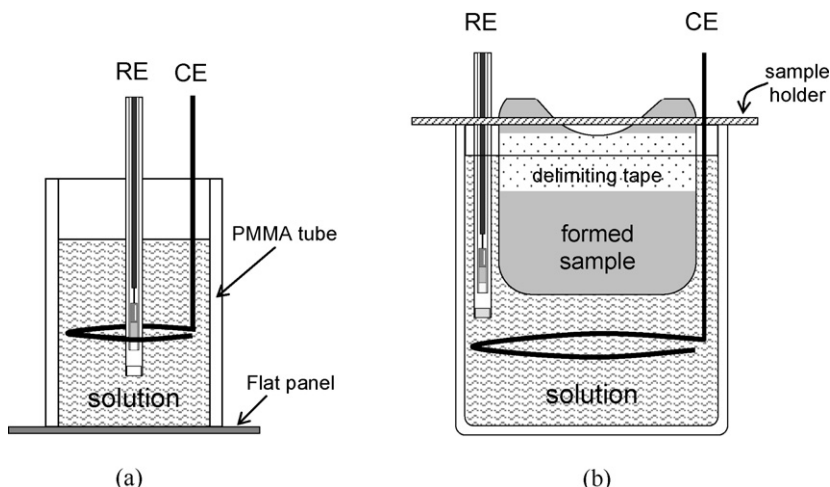


Fig. 2. Electrochemical cells used for EIS measurements on flat (a) and formed (b) samples. RE means reference electrode and CE is counter electrode.

2.2. Electrochemical impedance spectroscopy

Delimitation of the exposed area in the working electrodes was made either by pressing polymethylmethacrylate (PMMA) tubes with rubber o-rings against the surface (in the flat samples) or by applying insulating tape (formed samples). The exposed area was in both cases 46 cm^2 . The electrochemical study of the unpainted substrates was made only on flat samples, with an exposed area of 3.8 cm^2 . Painted samples were tested in 5 wt.% (0.86 M) NaCl and unpainted samples were tested in 0.1 M NaCl, prepared with *pro analysis* grade reagents and distilled water. A three-electrode arrangement was used, with a saturated calomel electrode as reference, a platinum counter electrode and the exposed sample area as working electrode (Fig. 2). The cell was connected to a Gamry PC4 +FAS1 Femtostat system and measurements were performed at room temperature, in a Faraday cage, with the solution quiescent and exposed to air. Each spectrum was obtained at open circuit potential, with a sinusoidal signal of 10 mV rms, in the frequency range 50 kHz–10 mHz or 1 mHz, depending on the stability of the system. Fitting of the spectra was made using ZView 2.70 software (Scribner Associates, USA), on six replicates for each type of sample. For the fitting analysis, capacitive-like behaviours were described as constant phase elements (CPE's or Q) with impedance given by $Z_Q = Y_0^{-1}(j\omega)^{-n}$, where Y_0 is the frequency independent admittance, n is the power of the CPE, ω is the angular frequency (in radians) and $j = \sqrt{-1}$. For $n = 1$ the impedance of the CPE corresponds to a pure capacitor, $Z_C = (j\omega C)^{-1}$, where C is the capacitance. In this work, we assumed the values of Y_0 to correspond to a pseudo-capacitance.

2.3. Scanning vibrating electrode technique (SVET)

SVET measurements were performed using instrumentation from Applicable Electronics Inc. on specimens with 2 mm \times 2 mm of area exposed to 0.1 M NaCl. The microelectrode had a platinum tip with a diameter of 20 μm and was made to vibrate at an average distance of 200 μm above the surface, with 20 μm of amplitude. Each scan comprised 20 \times 20 points.

2.4. Scanning electron microscopy

A Hitachi S-2400 scanning microscope (15–25 kV) coupled to a Rontec energy dispersive X-ray spectrometer (EDS) was used to perform the microscopic inspection.

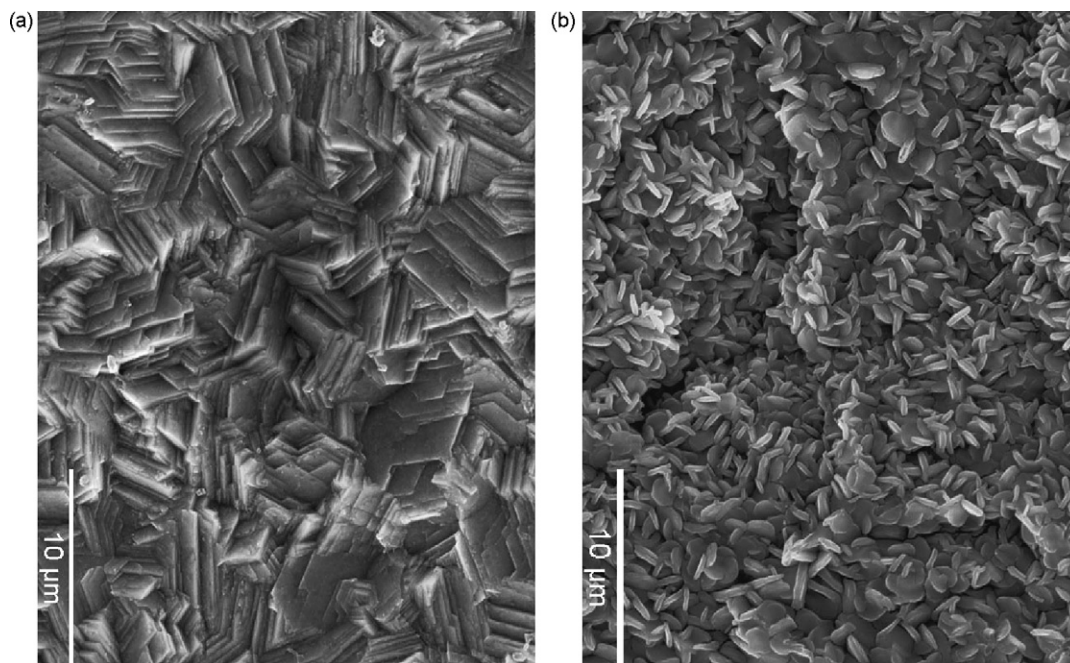


Fig. 3. Micrographs of electrogalvanised steel without pre-treatment, EG, (a) and after phosphating, PEG, (b).

3. Results and discussion

3.1. Bare substrates

The metal substrate had the typical morphology of zinc crystals randomly oriented resulting from electrodeposition, with an average crystal size of 3–5 µm, whereas the pre-treatment lead to good coverage with phosphate crystals of ~1 µm – Fig. 3.

Both substrates showed localised corrosion with the process growing in concentric circles (Fig. 4). In the case of electrogalvanised steel, corrosion remained in the initial regions, evolving in depth until steel was reached. Steel was galvanically protected by zinc and the anodic activity continued either by expanding the initial anodes or by nucleating at new locations. In the phosphated zinc the process started by localised attack of the phosphate layer with zinc oxidation on the exposed points, following a pattern similar to the non-phosphated substrate, although at a much slower rate.

The difference in corrosion resistance can be easily observed by SVET inspection of the surface. The attack of the surface occurs at small anodic spots scattered on a slightly cathodic surface, as observed by SVET mapping – Fig. 5. In contrast, the activity on the phosphated sample was negligible.

The impedance response of the electrogalvanised substrate corresponds to a process with two time constants, as revealed by two maxima in the phase angle plot (Fig. 6(a)). Starting from the high frequencies, a resistive response of ~100 Ω cm² corresponds to the uncompensated resistance between the working and reference electrodes, followed by a capacitive slope (due to the double layer, Q_{dl}) and a resistive plateau (charge transfer resistance, R_{ct}). The shift of the slope to lower frequencies reveals an increase of the pseudo-capacitance with time. This and the decrease of R_{ct} with time are consistent with the growth of the active area on the zinc surface, as the native oxide becomes dissolved as a consequence of local pH changes. The second time constant, detected at lower frequencies, was usually observed in the beginning of immersion, then disappeared after a few hours, and reappeared some days later. This is probably due to mass transport of charged species that occurs at the beginning, when the native surface oxide hinders the mass transport, but also at a later stage, when gel-like corrosion prod-

ucts over the surface represent a new obstacle to mass transport between the metal surface and bulk solution. Similar observation was made with pure zinc in the same environment [14]. On the phosphated substrate – Fig. 6(b) – the impedance was higher by

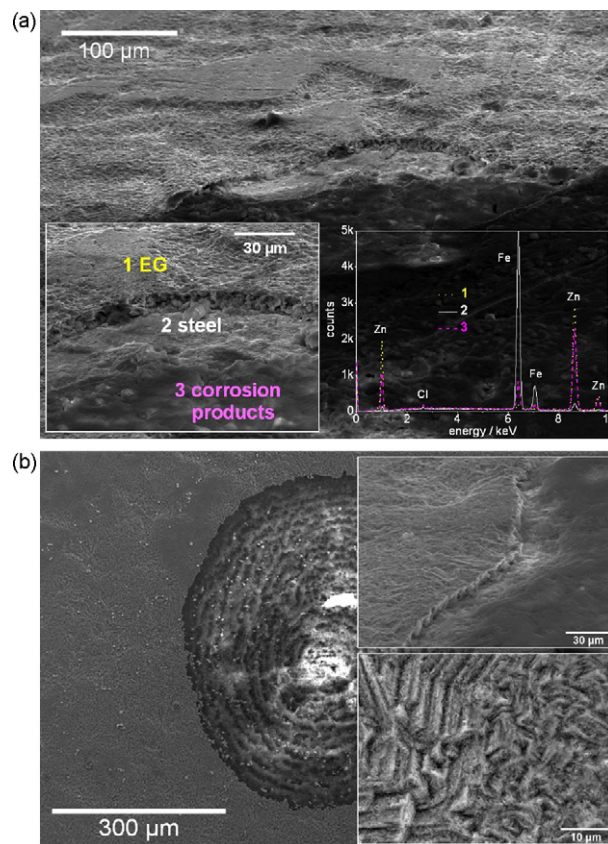


Fig. 4. Micrographs of EG (a) and PEG (b) after 3 days of immersion in 0.1 M NaCl. (a) Also shows EDS measurements on selected points of the surface and (b) shows magnified details of the border of the corroded spot and of the phosphate layer.

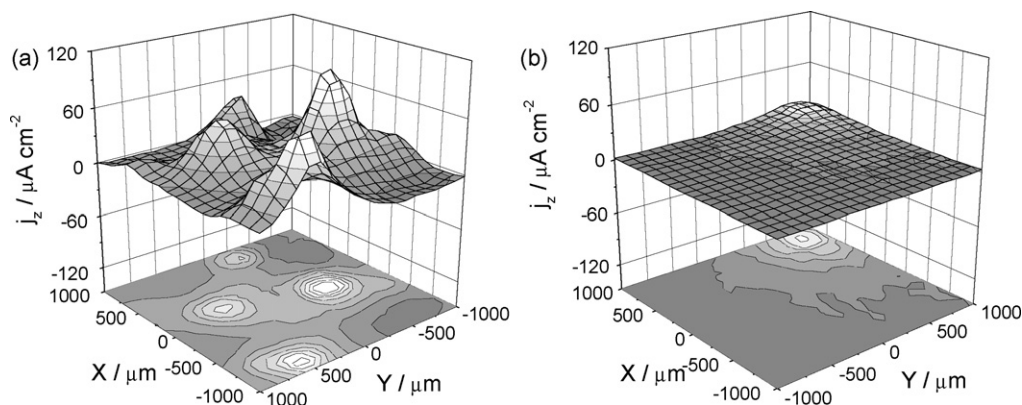


Fig. 5. Ionic current maps of non-phosphated (a) and phosphated (b) electrogalvanised steel after 4 h of immersion.

approximately two orders of magnitude. The low frequencies process is probably related to mass transport whereas the resistance at high frequencies is attributed to the solution resistance inside the pores of the phosphate layer. A third time constant at intermediate frequencies, visible in the 3 days spectrum, is attributed to corrosion of the metal substrate at the bottom of the pores. The phosphate layer is locally attacked due to pH variations [15], which results in an increase of the exposed area of the underlying zinc. With time, the high frequency time constant disappears and the corrosive process dominates the spectrum.

Interpretation of the substrate–solution interface can be made by equivalent electric circuits, introducing small variations as the system changes with time. According to our interpretation, the circuit in Fig. 7(a) describes the processes occurring on non-phosphated substrate, with the solution resistance, R_s , the double layer capacitance – numerically fitted as a CPE, Q_{dl} – and the charge transfer resistance R_{ct} . Mass transport was also present in some cases. The response of phosphated substrate in the first

hours of immersion has comparable elements, although Q_{phos} and R_{phos} stand for the capacitance of the phosphate layer and solution resistance inside the pores – Fig. 7(b). When the metal substrate becomes partially exposed and active, new elements – Q_{dl} and R_{ct} – account for the metallic corrosion – Fig. 7(c). Further degradation eventually leads to total activation, so that the circuit simplifies and becomes identical to that of the bare surface. In order to clarify the meaning of intermediate time constant, the unprotected area was intentionally increased by introducing an artificial scribe down to the zinc layer on a phosphated sample. In this situation, the high frequency time constant remained practically unchanged during the measured period, whereas the spectrum evolution at the intermediate frequencies revealed time growth of capacitance – Fig. 8 – identical to what was observed in the bare zinc surface. Fitting of the circuit for the degraded phosphate layer – in Fig. 7(c) – applied to a phosphated sample gave a good fitting and component values in the expected range, with Y_0 below $1 \mu\text{F cm}^2 \text{ s}^{n-1}$ for the phosphate layer and $\sim 12 \mu\text{F cm}^2 \text{ s}^{n-1}$ for the double layer – Fig. 9. The

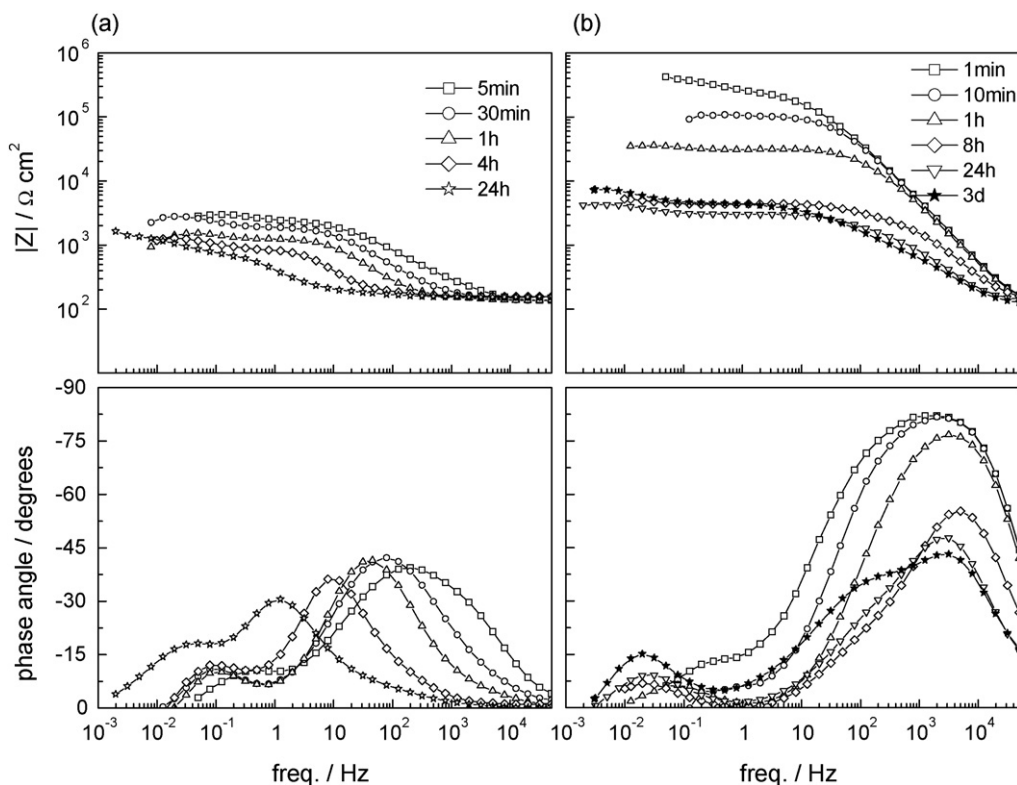


Fig. 6. Bode plots of EIS of electrogalvanised steel, EG (a) and phosphated electrogalvanised steel, PEG (b) in 0.1 M NaCl.

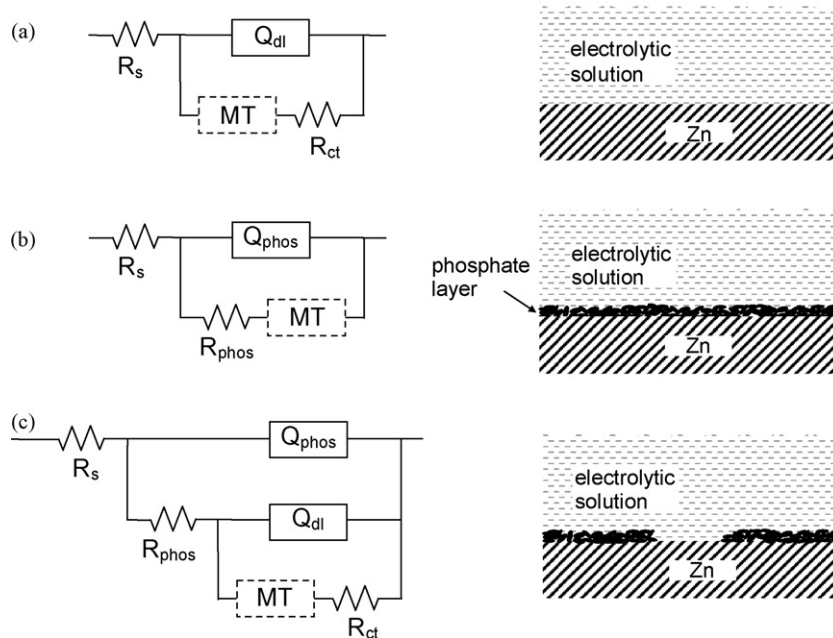


Fig. 7. Equivalent circuits and schematic representations of the corresponding interfaces: electrogalvanised steel (a); intact phosphated electrogalvanised steel (b); phosphated electrogalvanised steel under corrosion (c).

evolution of the electrochemical parameters obtained from fitting (Fig. 10) shows that the resistance of the solution inside the pores of the phosphate layer decreased rapidly during the first hours of immersion because of the fast ingress of solution across the pores. After a few hours, signs from activity on the metal surface were detected. R_{ct} was higher in phosphated samples because corrosion was limited to the discontinuities of the phosphate layer, where zinc was exposed. The decrease of R_{ct} and increase of $Y_{0,dl}$ both indicate an increase of active area. The higher capacitances and lower resis-

tances of EG show faster degradation compared to the phosphated substrate. The final value of $Y_{0,dl}$ on EG was very high for a double layer and can thus be due to the existence of corrosion products with conductive properties, which increased the electrochemically active area.

3.2. Painted samples

The EIS spectrum consists of the paint film response at the high frequencies and the corrosion process at the low frequencies. The exception to this is the first hours of immersion, when the response was dominated by the capacitive response – Fig. 11. With time the film resistance R_f decreased and the film capacitance C_f increased due to water uptake by the polymeric matrix, as given by

$$C_f = \frac{\epsilon_p \epsilon_0 A}{d}$$

where ϵ_p is the dielectric constant of the paint material, ϵ_0 is the permittivity of vacuum, A is the area and d is the film thickness. Typical values of polymer dielectric constants lie between 3 and 8 [16], significantly lower than the value of 80 reported for water at 20 °C [16]. Thus, water absorption by the paint results in a higher dielectric constant and in a higher capacitance. R_f decreased with time, indicating a gradual loss of barrier effect by increment of ionic species transported across the film between the environment and the metal surface. This was most likely accompanied by transport of water and oxygen. When R_f reached 10^7 – $10^8 \Omega \text{ cm}^2$, the first signs of activity on the metal were detected, giving a second capacitive response attributed to the double layer and a resistive response attributed to the charge transfer across the metal–solution interface. Yet, there is the possibility of a response from the phosphated layer before the appearance of the response of the metal surface. The evolution of the paint delamination from the metal substrate brings an increase in the wetted metal area and thus an increase in C_{dl} and decrease in R_{ct} . Degradation proceeds with the increment of capacitive parameters and decrease of resistive parameters. The faster evolution of the parameters for the non-pre-treated samples is clearly related to the higher degradation. These results contradict Shastry and Fountoulakis et al. [17] and Claus et

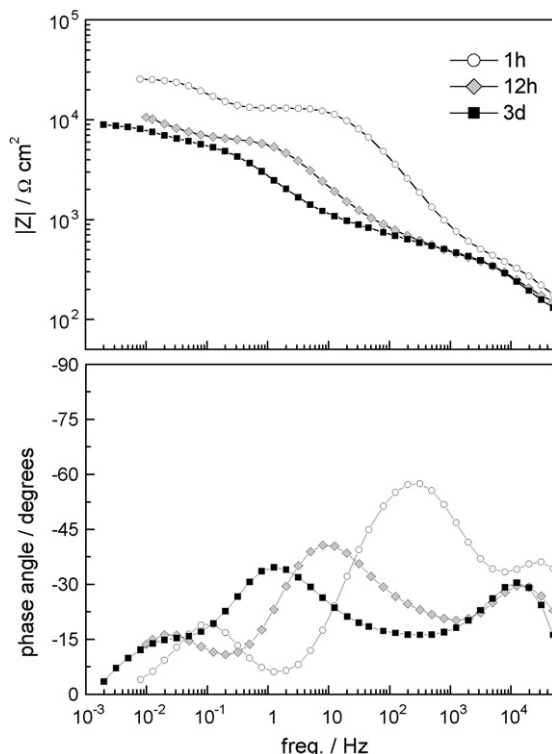


Fig. 8. Bode plots of EIS of scribed PEG immersed in 0.1 M NaCl.

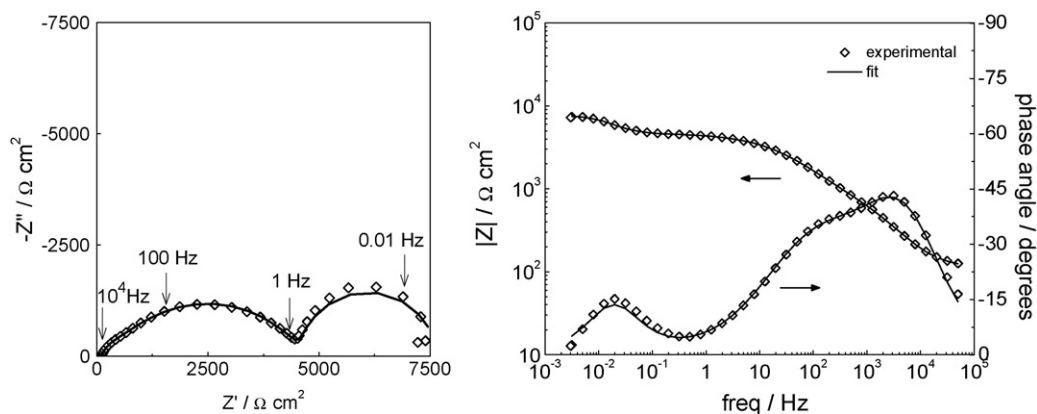


Fig. 9. Response of PEG after 3 days of immersion in 0.1 M NaCl fitted with circuit of Fig. 6(c). Parameters: $R_c = 119 \Omega \text{ cm}^2$; $Y_0(Q_{phos}) = 6.73 \times 10^{-7} \text{ F cm}^{-2} \text{ s}^{n-1}$; $n(Q_{phos}) = 0.847$; $R_{phos} = 6.94 \times 10^2 \Omega \text{ cm}^2$; $Y_0(Q_{dl}) = 1.17 \times 10^{-5} \text{ F cm}^{-2} \text{ s}^{n-1}$; $n(Q_{dl}) = 0.609$; $R_{ct} = 3.86 \times 10^3 \Omega \text{ cm}^2$; $Y_0(Q_{MT}) = 3.20 \times 10^{-3} \text{ F cm}^{-2} \text{ s}^{n-1}$; $n(Q_{MT}) = 0.954$; $R_{MT} = 3.01 \times 10^3 \Omega \text{ cm}^2$, $\chi^2 = 4 \times 10^{-4}$.

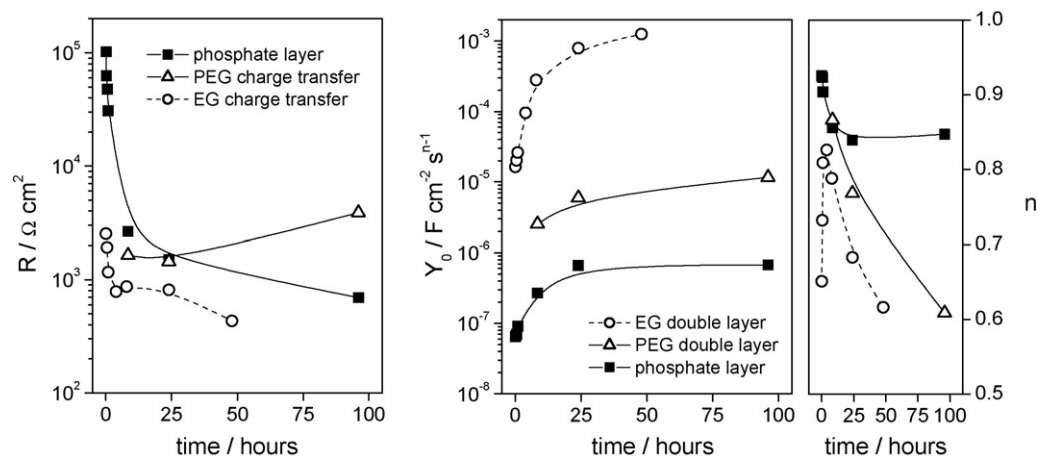


Fig. 10. Evolution of the electrochemical parameters related to the corrosion processes on electrogalvanised steel (EG) and phosphated electrogalvanised steel (PEG).

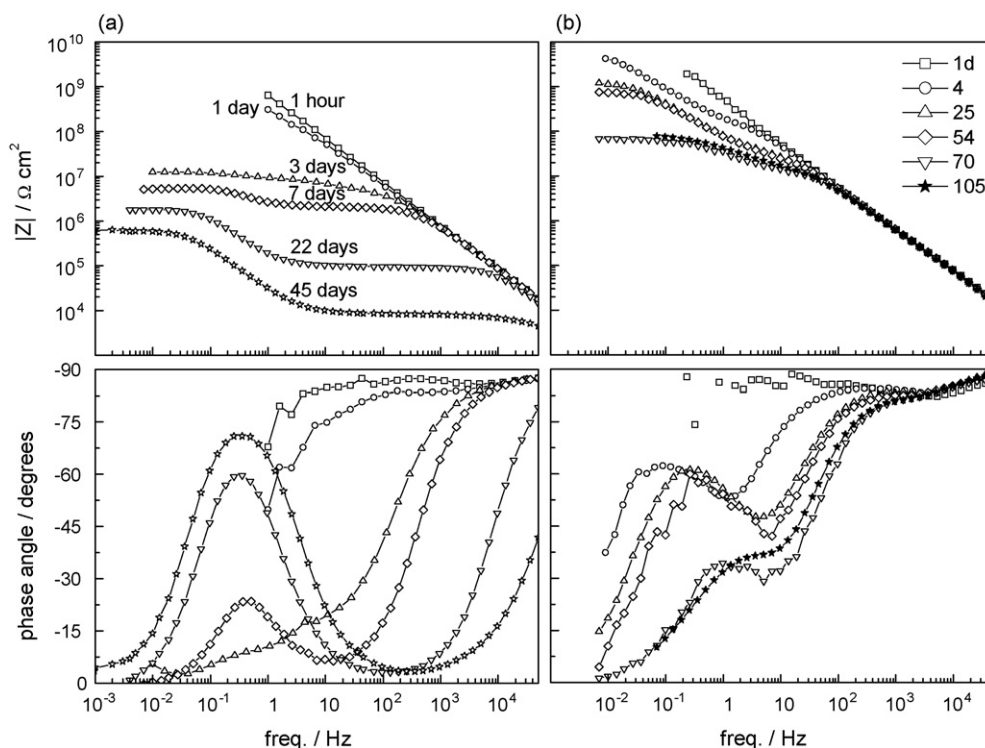


Fig. 11. Bode plots of EIS of flat painted samples without (a) and with (b) pre-treatment immersed in 5% NaCl.

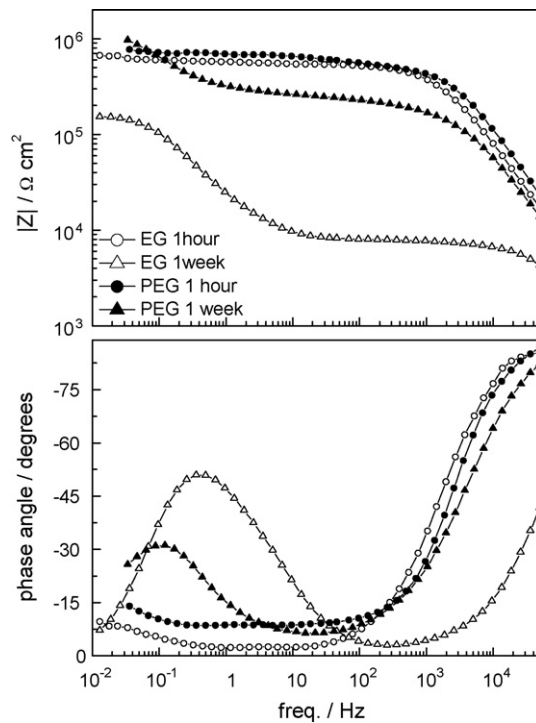


Fig. 12. Impedance response of formed painted samples with (PEG) and without (EG) pre-treatment after 1 h and 1 week of immersion in 5% NaCl.

al. [18], who found no significant difference between phosphated and unphosphated painted galvanised steel. In addition to promoting adhesion, the phosphate can give some corrosion resistance by impeding the contact of the underlying metal with the corrosive medium.

In the formed samples, the mechanical degradation suppressed the purely capacitive response in the first moments of immersion – Fig. 12. In a first stage, and despite the effects of forming on the underlying phosphate layer, the low frequency impedance is nearly the same for the pre-treated and the non-pre-treated sample, i.e., the impedance is that of the stretched organic coating. After that, loss of adhesion is faster in the non-phosphated sample, leading to significant drops of both coating resistance and charge transfer resistance.

Visual inspection of the samples after immersion corroborated the electrochemical results, with no signs of degradation in the flat pre-treated specimens – Fig. 13(a) and extensive delamination in the flat non-treated samples – Fig. 13(b). The shape of blisters in the formed samples varied with the pre-treatment. In the phosphated specimens, blisters were round-shaped, prominent and located preferentially in the most severely strained regions of the sample – Fig. 13(c–d) – whereas in the non-phosphated samples delamination was nearly complete, with wrinkling of the paint film, revealing extremely poor adhesion – Fig. 13(e).

The impedance data was numerically fitted using equivalent circuits. Fig. 14(a) presents the most used circuit to describe the impedance response of painted metals superimposed on a sketch of the system, in which the capacitance was replaced by a CPE, Q . When a third time constant appeared, the circuit in Fig. 14(b) was used, in which Q_{cp} and R_{cp} are attributed to a layer of corrosion products at the metal–coating interface [19]. Two types of corrosion products may exist, either a thin layer with some protective action or a thick layer of precipitated corrosion products. Fig. 14(c) shows the application of this circuit to the response of a formed non-pre-treated sample. The evolution of the paint film parameters is presented in Fig. 15. The capacitance of the film, described by Y_{0f} , apparently started from the same value, of $2 \times 10^{-10} \text{ F cm}^{-2} \text{ s}^{n-1}$, which corresponds to the capacitance of the dry film. Its value increased with time, at a faster rate in the

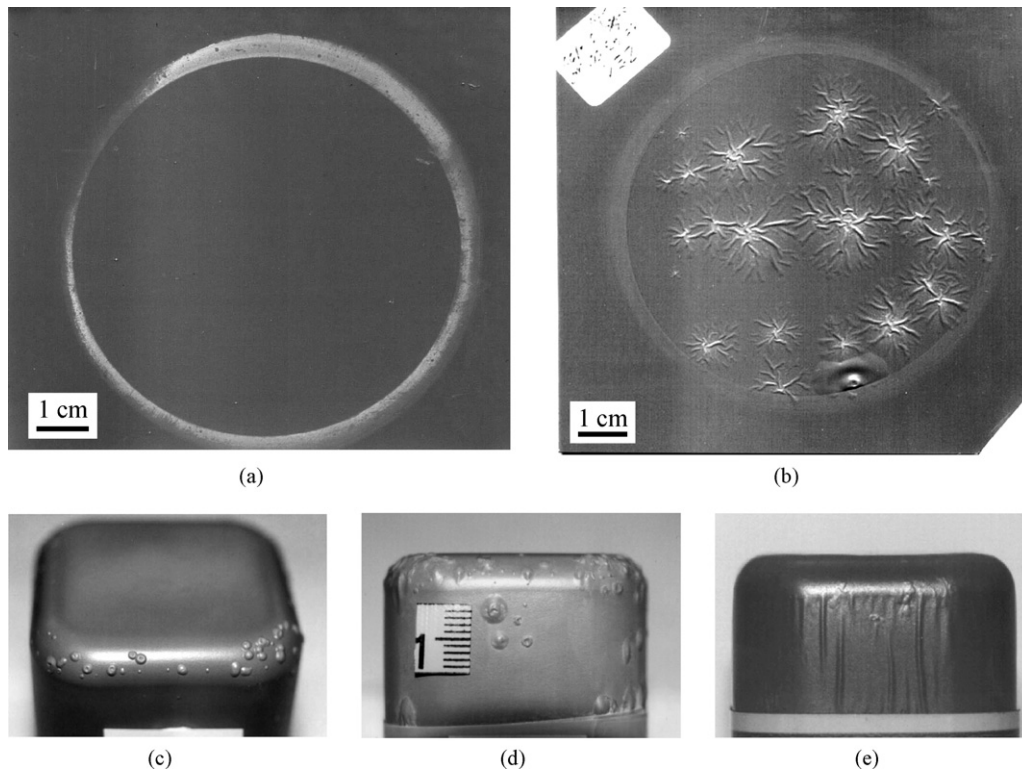


Fig. 13. Flat samples after immersion: pre-treated sample after 105 days (a) and sample without pre-treatment after 45 days (b). Formed samples after immersion: with pre-treatment after 10 days (c) and 22 days (d), without pre-treatment after 10 days (e).

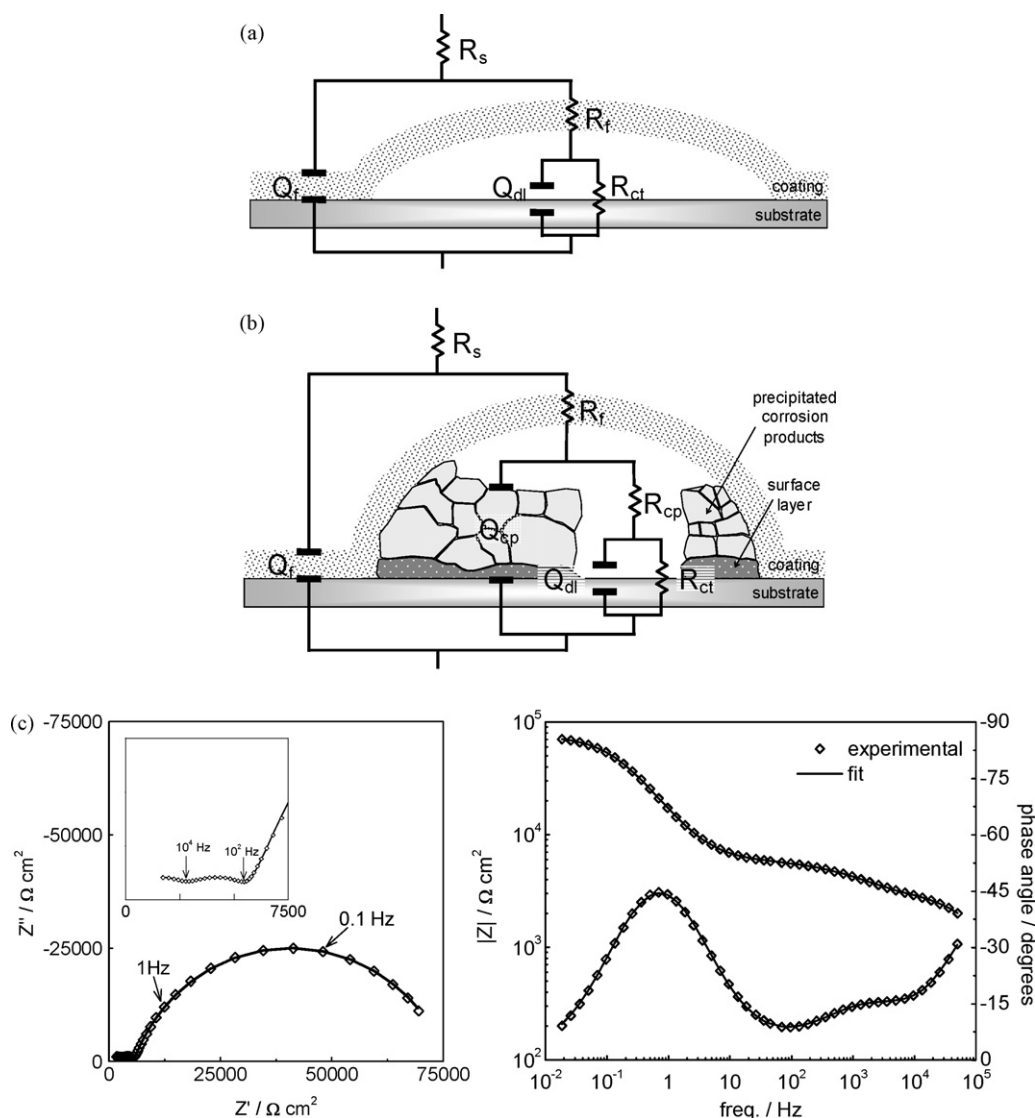


Fig. 14. Equivalent circuits used to fit the EIS results, (a) and (b); fit of spectrum obtained on a formed sample without pre-treatment after 37 days of immersion in 5% NaCl (c). Parameters: $R_s = 573 \Omega \text{ cm}^2$; $Y_0(Q_f) = 3.33 \times 10^{-9} \text{ F cm}^{-2} \text{ s}^{n-1}$; $n(Q_f) = 0.924$; $R_f = 2.16 \times 10^3 \Omega \text{ cm}^2$; $Y_0(Q_{dl}) = 1.14 \times 10^{-6} \text{ F cm}^{-2} \text{ s}^{n-1}$; $n(Q_{dl}) = 0.656$; $R_{ox} = 3.24 \times 10^3 \Omega \text{ cm}^2$; $Y_0(Q_{dl}) = 1.49 \times 10^{-5} \text{ F cm}^{-2} \text{ s}^{n-1}$; $n(Q_{dl}) = 0.797$; $R_{ct} = 7.01 \times 10^4 \Omega \text{ cm}^2$, $\chi^2 = 3 \times 10^{-5}$.

formed samples, whereas R_f decreased in all samples. The initial resistance of flat samples was above $10^9 \Omega \text{ cm}^2$, which represents a high barrier effect of the intact coating, while the barrier resistance of the stretched coating was only $10^6 \Omega \text{ cm}^2$. The resistance was always higher for the flat samples; further, in formed samples, the pre-treated samples had higher values except in $t=0$. The parameters related with the electrochemical activity on the metal surface, $Y_{0,dl}$ and R_{ct} , are plotted versus time of immersion in Fig. 16. $Y_{0,dl}$ was higher in the formed samples compared to the flat panels. For the same type of deformation, $Y_{0,dl}$ was always higher in the non-pre-treated samples. R_{ct} had the opposite variation: lower in formed samples and, when comparing the same type of deformation, lower in the non-pre-treated samples.

In terms of the electrochemical parameters, the effect of forming lead to the highest growth in capacitance and to the highest resistance drop. In fact, the resistance drop is of three orders of magnitude in the phosphated sample, compared to a drop of one order of magnitude in the non-phosphated sample. Further, the increase of capacitance is also more intense in the phosphated sample. This might suggest a more deleterious effect of forming on

the phosphated substrate. However, this large drop means in fact a change from total protection to a state of active corrosion at local defective areas, at which adhesion was lost. In the non-phosphated sample, delamination occurred even in flat material, and therefore the electrochemical measurable effect of deep drawing is less evident.

The influence of the various layers (electroplated, phosphate and organic film) to protect the steel was analysed in this work. The phosphate layer increased the anticorrosive properties by improving the paint adhesion and by offering an extra barrier to the aggressive corrosion medium. However, it was previously observed that strain diminished the action of phosphate coatings by originating cracks that expose the metal underneath [11]. When steel becomes exposed, its oxidation is prevented via galvanic protection by zinc. Mechanical deformation also introduces defects on the paint layer, most of them nucleated near the mineral constituents of the matrix (pigments and fillers) [11]. The extension of these defects is dependent on the type and level of strain. In fact, the morphology of attack on the formed cups varied according to the strain distribution on the cup, with the corners, i.e., the most strained regions, showing the higher degradation. The present work

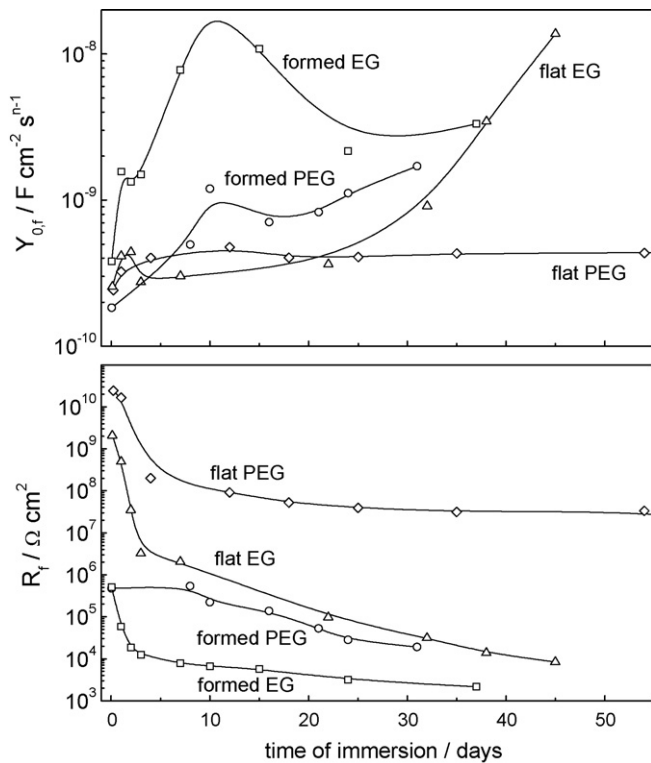


Fig. 15. Evolution with time of immersion of the electrochemical parameters related to the coating film of the formed and flat painted samples without pre-treatment (EG) and with pre-treatment (PEG).

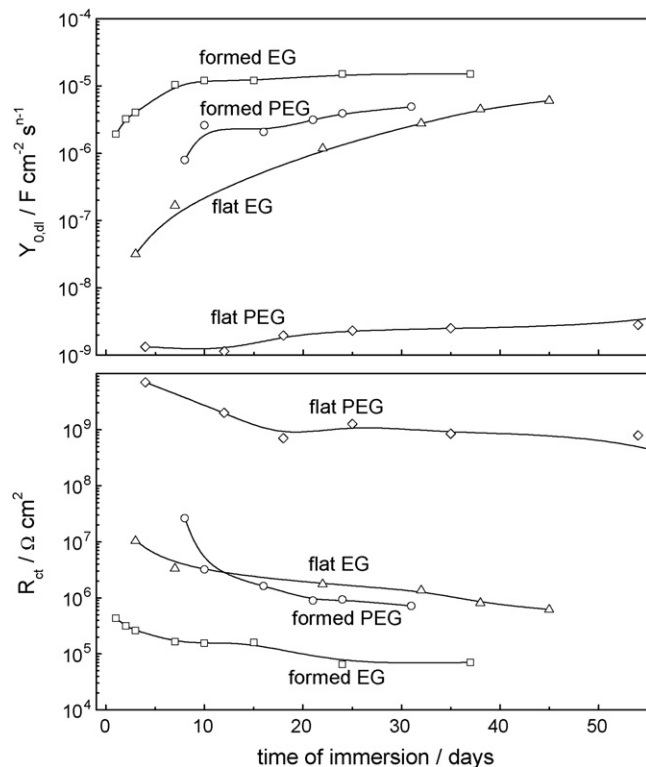


Fig. 16. Evolution with time of immersion of the electrochemical parameters related to the corrosion on the metal substrate in the formed and flat painted samples without pre-treatment (EG) and with pre-treatment (PEG).

just analysed the global response of the cups but it will be important to characterise the local response of the different regions.

4. Conclusions

The effect of mechanical deformation on the anticorrosive behaviour of pre-painted electrogalvanised steel was studied, on samples with and without phosphating pre-treatment. EIS provided parameters associated with the degradation of the paint system and the corrosion of the substrate, which were used to compare the performance of the different samples. Forming led to accelerated degradation, which can be assessed by the evolution of the electrochemical parameters. In a first stage, the impedance of the coated samples is controlled by the barrier properties of the coating even though the coating is highly strained. For longer immersion times, the charge transfer resistance drop caused by deep drawing was higher in the phosphated substrate due to the transition from a blocked surface to a blistered one. In the non-phosphated samples, deep drawing caused lower changes in the resistance and capacitance values, which nevertheless correspond to an actual acceleration of the corrosion process, under a totally delaminated coating.

Acknowledgements

We acknowledge funding from ECSC under the contract no. 7210-PD/189. We thank Prof. Guido Grundmeier (University of Paderborn) for useful discussions.

References

- [1] World Steel in Figures, 2003 edition, International Iron and Steel Institute, 2003.
- [2] J.F.H. van Eijnsbergen, Duplex Systems – Hot Dip Galvanizing plus Painting, Elsevier, Amsterdam, 1994.
- [3] J. Lange, A. Luisier, E. Schedin, G. Ekstrand, A. Hult, J. Mat. Proc. Technol. 86 (1999) 300.
- [4] H.Y. Kim, B.C. Hwang, W.B. Bae, J. Mat. Proc. Technol. 120 (2002) 290.
- [5] K. Ueda, H. Kanai, T. Suzuki, T. Amari, Prog. Org. Coat. 43 (2001) 233.
- [6] F. Deflorian, L. Fedrizzi, S. Rossi, Corros. Sci. 42 (2000) 1283.
- [7] V. Lavaert, P. Praet, M. Moors, E. Wettinck, B. Verheghe, Prog. Org. Coat. 39 (2000) 157.
- [8] M. Deluchi, A. Barbucci, G. Cerisola, Electrochim. Acta 44 (1999) 4297.
- [9] A.S. Castela, A.M.P. Simões, M.G.S. Ferreira, Mater. Sci. Forum 289–292 (1998) 247.
- [10] A.C. Bastos, A.M.P. Simões, Prog. Org. Coat. 46 (2003) 220.
- [11] A.C. Bastos, C. Ostwald, L. Engl, G. Grundmeier, A.M. Simões, Electrochim. Acta 49 (2004) 3947.
- [12] G. Bustamante, F.J. Fabri-Miranda, I.C.P. Margarit, O.R. Mattos, Prog. Org. Coat. 46 (2003) 84.
- [13] EN 10130:1991. Cold rolled low carbon steel flat products for cold forming. Technical Delivery Conditions.
- [14] A.C. Bastos, M.G.S. Ferreira, A.M. Simões, Prog. Org. Coat. 52 (2005) 339.
- [15] A. Amirudin, D. Thierry, Prog. Org. Coat. 28 (1996) 59.
- [16] J.A. Dean (Ed.), Lange's Handbook of Chemistry, 15th ed., McGraw-Hill Inc., New York, 1999.
- [17] C.R. Shastry, S.G. Fountoulakis, Proceedings of the Third International Conference on Zinc and Zinc Alloy Coated Steel Sheet (GALVATECH'95), Japan, 1995, p. 627.
- [18] G. Claus, Y. Houbaert, J. Dilewijns, U. Meers, M. Vanthournout, G. Verhoeven, Behaviour of pre-phosphated Zn-coated steel sheet during and after final phosphating, in: G. Krauss, D.K. Matlock (Eds.), Zinc-Based Steel Coating Systems: Metallurgy and Performance, The Minerals, Metals & Materials Society, 1990, p. 219.
- [19] S.F. Mertens, C. Xhoffer, B.C. Cooman, E. Temmerman, Corrosion (NACE) 55 (1999) 151.